Vortex-glass transitions in low-T_c superconducting Nb thin films and Nb/Cu superlattices

J. E. Villegas and J. L. Vicent
Departamento Fisica de Materiales, Facultad Fisicas, Universidad Complutense, 28040 Madrid, Spain
(Received 29 November 2004; revised manuscript received 2 February 2005; published 29 April 2005)

We have studied electrical transport properties in the mixed state of superconducting Nb thin films and Nb/Cu superlattices. Using a scaling analysis of $I-V$ characteristics, we have found evidence of a vortex-glass transition in these low-T_c systems. We have investigated the dimensionality of the glass transition in both the artificially anisotropic Nb/Cu superlattices and Nb thin films. The latter show up a three-dimensional glass transition, while for Nb/Cu superlattices we have found a dimensional crossover from a *quasi*-two dimensional to a *pure* two dimensional glass transition, which is governed by the coupling of Nb layers across Cu ones. The length and energy scales relevant to these behaviors will be discussed, and compared to that of high-T_c systems.

DOI: 10.1103/PhysRevB.71.144522 PACS number(s): 74.78.Fk, 74.25.Dw, 74.25.Op, 74.70.−b

I. INTRODUCTION

Vortex matter physics has called the attention of researchers in many fields, especially since the discovery of high-T_c superconductors (HTCS). The vortex state provides a perfect realm to study properties of liquid, crystalline, and glassy phases. A plethora of different phases is observed in the mixed state of HTCS,[1] induced by the interplay of vortex-vortex interaction, thermal fluctuations, different kinds of disorder, anisotropy, dimensional effects, etc.[2] But the essential characteristic of the phase diagram of HTCS is the existence of two different states: a magnetically irreversible zero-resistance state and a reversible state with dissipative transport properties. In the absence of disorder, as in clean single crystals, the former corresponds to a vortex-solid phase with topological order, and the latter to a vortex-liquid phase, both of them separated by a first-order melting transition.[1] In the presence of strong *quenched* disorder, however, the long-range topological order of the vortex lattice is lost, and the zero-resistance state corresponds to a vortex glass (VG) instead to a vortex solid. The VG presents long-range superconducting phase coherence (zero resistance), and the transition into the dissipative liquid state becomes a continuous second-order phase transition.[3,4]

For conventional low-T_c superconductors (LTCS), the magnetic and electrical properties in the mixed state were mainly explained in the frame of flux-creep theories,[5] in which the existence of different phases was not considered. After the rich phenomenology of vortex phases came out with HTCS, LTCS have been seldom revisited to check the possible application of HTCS paradigms. Experimental evidence of a first order melting transition in Nb single crystals has been reported by several authors.[6–9] Studies on the VG transition in LTCS have not been made except for some limited systems, like In thin films,[10] or alloys as Mo_3Si,[11] and a-Mo_xSi_{1-x}.[12] In the case of Nb thin films, for example, the existence of a glass transition remains controversial[13,14] although, recently, Sun *et al.*[15] have observed glassy vortex dynamics in experiments of magnetic relaxation in Nb thin films with magnetic pinning centers.

In this paper, we report on the observation of VG transitions in Nb thin films and Nb/Cu superlattices. The VG transition has been investigated by measuring $I-V$ characteristics in magnetic fields applied perpendicular to the film plane. Those characteristics have been collapsed, according to the scaling rules proposed in the VG theory, in terms of critical exponents.[4] Such scaling analysis has been thoroughly applied to a number of HTCS systems earlier. However, Strachan *et al.*[17] have recently probed that the scaling of $I-V$ curves may not suffice to prove the occurrence of a VG transition, and have proposed additional criteria to ensure the existence of such transition. Moreover, in this work[17] it is pointed out that many of the data on the VG transition in HTCS reported so far do not meet the proposed criteria, and therefore is such cases the existence of a VG transition might be questionable. We have found that the data presented here for LTCS do fulfill the criteria proposed by Strachan *et al.*,[17] as we will show later.

We have studied the dimensionality of the VG transition as a function of the sample anisotropy. The artificially layered structure of the Nb/Cu superlattices has allowed tailoring the anisotropy in a controllable fashion, since the coupling of Nb layers through the Cu spacer can be easily tuned.[16] We have observed that Nb thin films show up a three dimensional (3D) VG transition, while Nb/Cu superlattices show a crossover from a *quasi*-two dimensional (2D) into a *pure* 2D VG transition, which is governed by the coupling of Nb layers in the superlattice. We will discuss on this crossover in terms of the relevant length scales. The phenomenology reported here for this artificially layered LTCS system is very similar to that observed for many HTCS systems: on one hand the values of the critical exponents found in the scaling analysis agree with that previously reported for HTCS. On the other because of the existence of a dimensional crossover governed by the anisotropy. We believe that these findings extents the universality of the VG transition.

II. EXPERIMENT

Nb thin films (100 nm thick) and Nb/Cu superlattices were grown on Si substrates using dc magnetron sputtering at room temperature in Ar atmosphere. Several series of superlattices $Cu_{d_{Cu}}[Nb_{d_{Nb}}/Cu_{d_{Cu}}]_N$ were grown, with a number

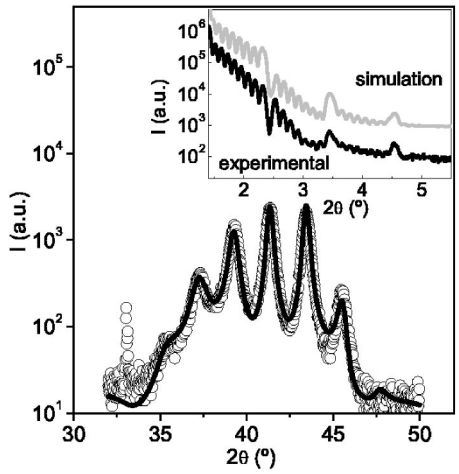

FIG. 1. High-angle x-ray diffraction spectra of sample $Cu_{2.5\ nm}[Nb_{1.8\ nm}/Cu_{2.5\ nm}]_8$ Open circles are experimental data, and the solid line is the refinement using the SUPREX program. Inset: Low-angle x-ray diffraction spectra of sample $Cu_{2.5\ nm}[Nb_{5.3\ nm}/Cu_{2.5\ nm}]_8$ Lower curve is the experimental one, and upper curve a simulation with SUPREX.

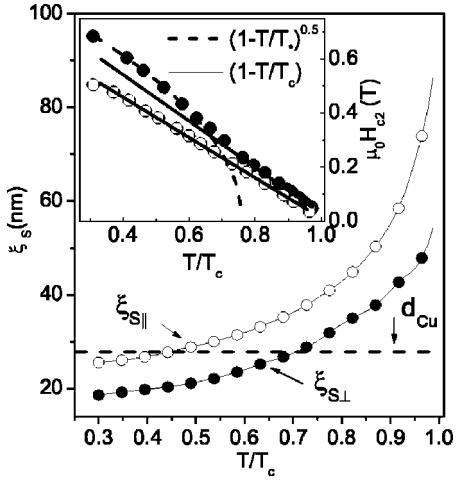

FIG. 2. Superconducting coherence lengths of sample $Cu_{27\ nm}[Nb_{13\ nm}/Cu_{27\ nm}]_{10}$ as a function of temperature, both parallel $\xi_{S\|}(T)$ and perpendicular $\xi_{S\perp}(T)$ to Nb/Cu layers. The horizontal dashed line marks the Cu thickness d_{Cu}. Inset: Measured parallel (black circles) and perpendicular (open circles) critical fields H_{c2}. Solid lines are linear fits $H_{c2\perp}(T) \propto (1-T/T_c)$, while the dashed one is the best fit to $H_{c2\|}(T) \propto (1-T/T_*)^{\alpha}$, with $\alpha = 0.49 \pm 0.02$ and $T_*/T_c = 0.75 \pm 0.01$.

N of bilayers such that sample thickness was always around 300 nm. Structural characterization was made by x-ray diffraction (XRD) techniques, both low-angle incidence XRD (LAXRD) and high-angle incidence (HAXRD). HAXRD showed that Cu layers are oriented (111), while Nb ones are (110). An example of the obtained HAXRD spectra is depicted on Fig. 1. As can be seen, superlattice peaks appear for scattering angles 2θ such that $2\Lambda \sin(\theta) = n\lambda$, where Λ is the modulation length of the superlattice (bilayer thickness, $\Lambda = d_{Nb} + d_{Cu}$), λ is the x-ray wavelength ($\lambda_{k_{Cu}} = 0.154\ 03$ nm), and n is an integer. The width of those superlattice peaks is related to structural disorder. We have refined the spectra using SUPREX[19] program. From refinements we obtained the modulation length Λ as well as the individual layer thickness d_{Nb} and d_{Cu}, and also quantified the several sources of disorder at the Nb/Cu interfaces, like interface roughness or interdiffusion.[19] The samples studied here did not present interdiffusion, and have moderate roughness at the interfaces, ranging from 0.2 to 0.6 nm, being larger the thicker the Nb layers are. These structural properties are similar to those reported earlier by other authors for the same system.[18] Experimental LAXRD spectra were compared to simulations, which were obtained with SUPREX (for an example, see the inset of Fig. 1). The parameters we get from these simulations (modulation lengths and disorder parameters) agreed with the results obtained from refinements of HAXRD, and confirmed the high structural quality of samples.

For magnetotransport experiments, samples were lithographed using wet etching into a measuring bridge 1 mm long and 100 μm wide with the standard four-probe configuration. Experiments were made in a liquid He cryostat provided with a superconducting solenoid. In all experiments temperature was controlled with stability of 1 mK.

III. RESULTS AND DISCUSSION

The superconducting coherence lengths $\xi_S(T)$ as a function of temperature were calculated from the upper critical fields $H_{c2}(T)$. These were obtained from magnetoresistance measurements at constant fixed temperatures $R(H)_T$, and using the criterion $R[H_{c2}(T)] = 0.95R_n$, with R_n the normal-state resistance just above T_c. The in-plane coherence length $\xi_{S\|}$ (parallel to Nb/Cu interfaces in the superlattices) and the perpendicular one $\xi_{S\perp}$ have been calculated by using $\xi_{S\|}(T) = [\phi_0 2\pi H_{c2\perp}(T)]^{1/2}$ and $\xi_{S\perp}(T) = \{\phi_0 H_{c2\perp}(T)/2\pi[H_{c2\|}(T)]^2\}^{1/2}$, respectively.[16] As an example, the behavior observed for sample $Nb_{13\ nm}/Cu_{27\ nm}$ is shown in Fig. 2. For this superlattice, the perpendicular critical field displays linear dependence on temperature $H_{c2\perp}(T) \propto (1-T/T_c)$ (see the inset of Fig. 2). However, the parallel critical field shows up a crossover from linear dependence $H_{c2\|}(T) \propto (1-T/T_c)$ at high enough temperatures to square-root $H_{c2\|}(T) \propto (1-T/T_c)^{1/2}$ at lower temperatures. This is indeed the signature of a dimensional crossover,[16] which takes place when the perpendicular coherence length $\xi_{S\perp}(T)$ reaches a value $\xi_{S\perp}(T) \sim d_{Cu}$ (thickness of Cu in the superlattice). This can be checked in the main panel of Fig. 2. More precisely, for temperatures such that $\xi_{S\perp}(T) > 0.7d_{Cu}$, the Nb layers are coupled through the Cu ones because of proximity effect. At temperatures below the crossover temperature ($T_{2D} \approx 0.5T_c$ for this superlattice) the coherence length is $\xi_{S\perp}(T) < 0.7d_{Cu}$, and therefore the Nb layers are decoupled, showing up 2D behavior.[16] For some other of the studied superlattices, as for instance $Nb_{3.4\ nm}/Cu_{2.4\ nm}$, $\xi_{S\perp}(T) > d_{Cu}$ at all temperatures, and thus such superlattices are always in the coupled regime. Coherence lengths at 0 K, $\xi_S(0)$, together with critical temperatures and other basic parameters of samples are listed in Table I.

TABLE I. Basic superconducting properties and VG scaling parameters of some of the studied samples. ρ is the in-plane resistivity just above T_c. Penetration depth at 0 K, $\lambda(0)$, has been estimated as in Ref. 31, by using Gorkov's theory $\lambda_\perp(0)=1.29\cdot10^{-2}(\rho/T_C)^{1/2}$ and $\lambda_\parallel=\varepsilon\lambda_\perp$. h is defined as $h\equiv H/H_{c2}(T_g)$.

Sample	T_c (K)	ρ ($\mu\Omega$ cm)	$\xi_{S\perp}(0)$ (nm)	$\xi_{S\parallel}(0)$ (nm)	$\lambda(0)_\parallel$ (nm)	Scaling parameters						
						$\mu_0H(T)$	h	T_g	D	z	ν	c_L
$Nb_{100\ nm}$	8.264	60	10	10	340	0.0085	0.24	8.194	3	4.2	1.6	0.032
						0.017	0.24	8.152	3	4.2	1.6	0.031
$Nb_{3.4\ nm}/Cu_{2.5\ nm}$	2.960	25	10	18	210	0.02	0.14	2.545	2	3.7	1.7	0.011
						0.05	0.22	2.280	2	4.1	1.7	0.013
						0.1	0.35	2.150	2	4.0	1.4	0.017
$Nb_{6\ nm}/Cu_{27\ nm}$	1.800	8	41	51	212	0.01	0.66	1.650	2	4.0	1.9	0.012
						0.02	0.71	1.501	2	4.0	1.9	0.014
$Nb_{13\ nm}/Cu_{27\ nm}$	4.850	9	15	21	125	0.11	0.73	3.994	2	4.0	2.0	0.024
						0.4	*Pure* 2D VG $T_g=0$					

We have measured $I-V$ characteristics with the magnetic field H applied perpendicular to film plane (i.e., perpendicular to Nb/Cu layers in the superlattices). For each fixed value of applied field H, we measured a set ($\sim$20) of isothermal $I-V$ curves at decreasing temperatures, as those shown in Figs. 3(a), 4(a), and 5(a). For all samples and applied magnetic fields the results are qualitatively similar. The isotherm at the highest temperature displays linear behavior at all current levels, with Ohmic resistance $R=V/I\approx R_n$. i.e., at this temperature $H=H_{c2\perp}$. For characteristics at slightly lower temperatures, the Ohmic response is observed only up to a threshold current level I_{nl}, above which the curves are nonlinear [black dots $V(I_{nl})$ in Figs. 3(a), 4(a), and 5(a)]. The Ohmic resistance in the low-current limit $\lim_{I\to0} V/I\neq0$ is

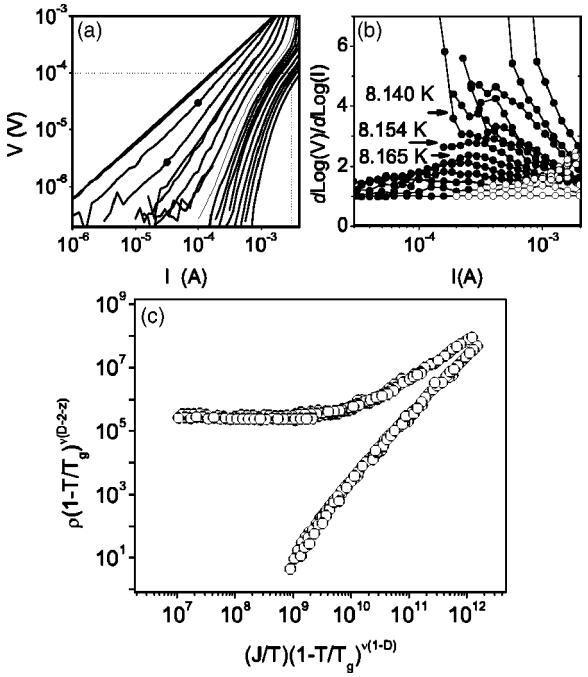

FIG. 3. (a) $I-V$ isotherms for a $Nb_{100\ nm}$ thin film in applied field $\mu_0H=0.017$ T at temperatures (from left to right) 8.220 K $>T>$ 8.004 K, separated $\sim$5–15 mK. Vertical and horizontal dotted lines delimit the experimental window used for scaling. Black dots are $V(I_{nl})$ (see text). (b) Derivatives of the log(V)-log(I) curves at temperatures (from bottom to top) 8.220 K $>T>$ 8.004 K. Black dots are within the experimental window used for scaling. Derivatives for isotherms around T_g are marked with arrows. (c) Scaling of the earlier isotherms as explained in the text.

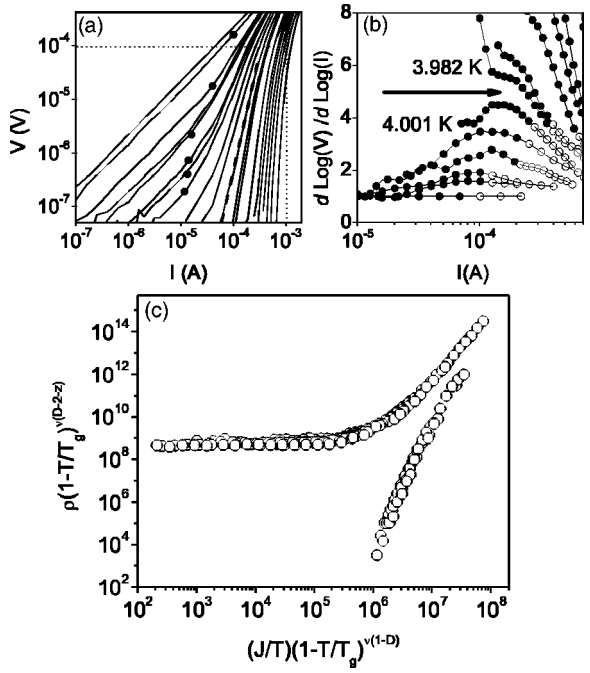

FIG. 4. (a) $I-V$ isotherms for sample $Cu_{27\ nm}[Nb_{13\ nm}/Cu_{27\ nm}]_{10}$ in applied field $\mu_0H=0.11$ T at temperatures (from left to right) 4.060 K $>T>$ 3.865 K, separated $\sim$5–15 mK. The dashed line separates isotherms above and below $T_g=3.994$ K. Vertical and horizontal dotted lines delimit the experimental window used for scaling. Black dots are $V(I_{nl})$ (see text). (b) Derivatives of the log(V) − log(I) curves at temperatures (from bottom to top) 4.060 K $>T>$ 3.908 K. Black dots are within the experimental window used for scaling. The arrow separates derivatives of isotherms just below and above T_g. (c) Scaling of the earlier isotherms as explained in the text.

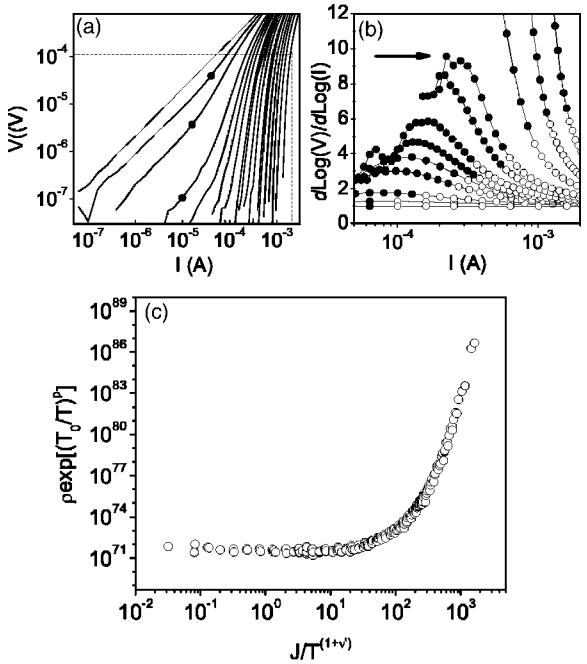

FIG. 5. (a) $I-V$ isotherms for sample $Cu_{27\ nm}[Nb_{13\ nm}/Cu_{27\ nm}]_{10}$ in applied field $\mu_0 H=0.4$ T at temperatures (from left to right) $2.160\ \mathrm{K}>T>1.780$ K, separated $\sim 5-15$ mK. Horizontal dotted line delimit the experimental window used for scaling. (b) Derivatives of the $\log(V)-\log(I)$ isotherms at temperatures (from bottom to top) $2.160\ \mathrm{K}>T>1.856$ K. Black dots are within the experimental window used for scaling. The arrow marks derivative of the isotherm at the lowest temperature among those showing decreasing slope in the low current limit. (c) Scaling of the isotherms shown in (a) with a *pure* 2D VG model.

smaller as the temperature decreases, as well as the onset of nonlinear response I_{nl} shifts to lower current levels as temperature is reduced. Below a given temperature, isotherms become highly nonlinear within the whole experimental window, and show up negative curvature in the low-current limit yielding zero resistance $\lim_{I\to 0} V/I=0$.

The phenomenology described earlier suggests the existence of a continuous transition from a truly superconducting phase with zero-resistance (VG) to a vortex-liquid dissipative phase closer to H_{c2}. As proposed by Fisher *et al.*,[3,4] and experimentally proved early for HTCS,[20] this glass transition is a second order transition in whose vicinity the related physical quantities must scale with the VG correlation length ξ_{VG} and a characteristic relaxation time τ. These two magnitudes diverge as temperature approaches the glass transition temperature T_g, following $\xi_{VG}\propto(T-T_g)^{-\nu}$ and $\tau\propto(T-T_g)^{-z\nu}$, with z and ν the dynamic and static critical exponents. Scaling laws have been proposed to collapse onto a single master curve all $I-V$ (or $E-J$) isotherms within the critical region, by means of the ansatz:[4]

$$E\xi_{VG}\tau \approx J\xi_{VG}^{D-1}\zeta_{\pm}(J\phi_0\xi_{VG}^{D-1}k_BT), \tag{1}$$

where D is the dimensionality of the glass transition, $\zeta_{\pm}$ is a universal scaling function above (ζ_+) or below (ζ_-) T_g, ϕ_0 is the flux quantum, and k_B is the Boltzmann constant. We have applied this scaling analysis to measured $I-V$ characteristics within the experimental window $10^{-8}\ \mathrm{V}<V<10^{-4}$ V and $I<2\cdot 10^{-3}$ A. If injected currents are too high, the system is driven towards free flux flow, where the scaling analysis is no longer valid.[17,21,22] Thus we set the voltage cutoff at 10^{-4} V, since above this all characteristics deviated towards Ohmic behavior. This can be seen in Figs. 3(b), 4(b), and 5(b), where the slopes of the isotherms $d(\log V)/d(\log I)$ are displayed.

For the Nb thin film and Nb/Cu superlattices whose Nb layers are coupled [superlattices with $\xi_{S\perp}(T)>d_{Cu}$], the scaling analysis yielded good collapses, as those shown in Figs. 3(c) and 4(c), respectively. The parameters D, z, ν, and T_g obtained from scalings are listed on Table I, for the different samples and applied magnetic fields H. For the Nb thin film it was found $D=3$, which corresponds to a three dimensional VG transition. The critical exponents were around $z\approx 4.2$ and $\nu\approx 1.6$. For all coupled Nb/Cu superlattices, the dimensionality was found to be $D=2$, which corresponds to a *quasi*-bidimensional (*quasi*-2D) VG transition. The results about dimensionality will be discussed later in this paper. The critical exponents for coupled superlattices were around $z\approx 4$ and $\nu\approx 1.8$. These parameters were not either magnetic field or sample dependent and, as those found for Nb thin films, are always within the range $z\approx 4-6$ and $\nu\approx 1-2$ predicted by the theory.[4] Furthermore, we want to underline that the values obtained here for LTCS are very similar to that observed for 3D and *quasi*-2D VG transitions in HTCS: for instance, those found for 3D VG transitions in optimally oxygenated $YBa_2Cu_3O_{7-\delta}$ thin films,[20,21,24,26] and for *quasi*-2D VG transitions in $Bi_2Sr_2Ca_2Cu_3O_x$,[23] oxygen depleted $YBa_2Cu_3O_{7-\delta}$[24] and a-axis oriented $EuBa_2Cu_3O_{7-\delta}$ thin films.[25] This suggests that the VG transitions found here for LTCS belong to the same universality than those of HTCS.

Recently, however, Strachan *et al.*[17] have proved that the scaling method used might be misleading, even if it yields universal values of the critical exponents. They have argued that experimental limitations related to the voltage sensitivity floor might allow achieving good collapses with arbitrary values of some of the scaling parameters, as for instance T_g. Thus, Strachan *et al.*[17] have proposed that a criterion to unambiguously determine T_g should be met: isotherms above and below T_g, but with equal $|(T-T_g)/T_g|$, must have opposite concavities at the same applied current level. In order to ensure that the scaling analysis applied is correct, we have checked the accomplishment of this criterion for every set of $I-V$ curves that were successfully scaled. To this end, we have calculated the derivatives $d(\log V)/d(\log I)$ of the $I-V$ isotherms. In Figs. 3(b) and 4(b) we show the derivatives of the $I-V$'s depicted in Figs. 3(a) and 4(a), respectively. As can be seen in Fig. 3(b), the Nb data met the outlined criterion: at the lowest current levels, upward ($T=8.140$ K), and downward ($T=8.165$ K) slopes are observed for isotherms at similar distance $|(T-T_g)/T_g|$ below and above $T_g=8.152\pm 0.002$ K (obtained from the scaling analysis). The isotherm at $T=8.154$ K is indeed the critical isotherm itself, or lies closely just above. Such characteristic displays a slope

around ~2.6 in the low-current limit. This value is actually expected from the VG theory and the values of the critical exponents obtained from the scaling. Following Fisher *et al.*,[4] the isotherm at T_g fulfills the relation $E \propto J^{\alpha+1}$ in the low-current limit, where $\alpha=(z+2-D)/(D-1)$. Therefore, using the values obtained in our scaling, $D=3$ and $z=4.2\pm0.1$, the expected slope of the critical isotherm would be $\alpha+1=2.6\pm0.05$, which agrees with the value extracted from the derivatives. Also the data for a Nb/Cu superlattice shown in Fig. 4 fulfill the earlier criteria. From the scaling in Fig. 4(c) we obtained $T_g=3.994\pm0.002$ K for the set of isotherms in Fig. 4(a). As can be seen in the derivatives of Fig. 4(b), the isotherms above ($T=4.001$ K) and below ($T=3.982$ K) this temperature show opposite curvatures in the low-current limit. Also, although the critical isotherm is not within the set of measured characteristics, we can give lower and upper limits to its slope from those of the isotherms just above and below T_g. As can be seen in the same Fig. 4(c), the first isotherm below T_g ($T=3.982$ K) has a slope larger than ~5.5 in the low-current limit, whilst the first one above T_g ($T=4.001$ K) displays a slope smaller than ~4.5. Therefore, the critical isotherm in between them should have a slope around ~4.5–5.5. This agrees with the value expected from scaling parameters $D=2$ and $z=4.0\pm0.1$, yielding $\alpha+1=(z+2-D)/(D-1)+1=5\pm0.1$

The behavior of superlattices whose Nb layers were decoupled was investigated too. To this end, we have measured $I-V$ characteristics of sample $Nb_{13\ nm}/Cu_{27\ nm}$ in applied magnetic field $\mu_0 H=0.4$ T. For this field, all $I-V$'s were measured at temperatures well below $T=T_{2D}\approx 0.5T_c$, and therefore $\xi_{S\perp}(T)<0.7d_{Cu}$ (see Fig. 2). The $I-V$'s are depicted in Fig. 5. For these isotherms, however, the scaling rule [Eq. (1)] did not allowed obtaining collapses as the ones obtained in the coupled regime $\xi_{S\perp}(T)>0.7d_{Cu}$ In fact, from the derivatives of the $I-V$ curves [Fig. 5(b)], one can observe some features that rule out the scaling of those isotherms according to a *quasi*-2D or 3D VG transition. On one hand, it is not possible determining a finite T_g using the criterion outlined earlier, since two isotherms of opposite concavities at the same current level cannot be found. Even though this might occur just because the voltage sensitivity floor truncates the isotherms, another piece of evidence allows discarding a *quasi*-2D or 3D VG transition in the decoupled regime: as can be seen in Fig. 5(c), a maximum slope around ~9 is displayed by the isotherms showing up a decreasing slope in the low current limit. This is marked with an arrow in Fig. 5(b). Using the criterion of Strachan *et al.*, the isotherm at T_g should be above this one in Fig. 5(b) (i.e., at a lower temperature), and therefore it should have a slope larger that ~9. As we said before, in a *quasi*-2D or 3D VG transition the slope of the critical isotherm is $\alpha+1=(z+2-D)/(D-1)+1$, which would imply a critical exponent $z>8$ for $D=2$, or $z>17$ if $D=3$. These are very high values of the critical exponents, not supported by the theory.[4] As argued earlier,[28,29] this fact strongly suggests that a *quasi*-2D or 3D VG transition has to be dismissed. However, a good scaling of the isotherms in Fig. 5(a) is achieved by assuming a different *pure* 2D VG transition, as proposed by Dekker *et al.*,[27] and found later in highly anisotropic HTCS systems.[24,28,29] In a *pure* 2D VG transition, the glass transition temperature $T_g=0$. Therefore, a *pure* 2D VG phase does not exist at any finite temperature, although in-plane (2D) correlations develop, diverging as $\xi_{VG} \propto 1/T^{\nu'}$ when temperature approaches $T_g=0$. In this transition, the scaling of the isotherms is achieved by plotting $\rho \exp[(T_0/T)^p]$ vs $J/T^{1+\nu'}$, where $\rho=E/J$ is the resistivity, T_0 is a characteristic temperature, and p and $\nu'=2$ are characteristic exponents of the *pure* 2D VG transition. The exponent p is related to the mechanism of vortex motion: $p \geqslant 1$ for thermal activation over the relevant energy barriers, whereas $p \approx 0.7$ is expected in the case of quantum tunneling across them.[27] As can be seen in Fig. 5(c), a good collapse has been obtained with parameters $T_0=300\pm20$ K, $p=1.05\pm0.02$, and $\nu'=2$.

Let us now discuss on the meaning of dimensionality in the different behaviors observed so far. The Nb thin film shows up a 3D VG transition within the range of applied magnetic fields investigated. On the other hand, Nu/Cu superlattices show up *quasi*-2D or *pure* 2D VG transitions, as those found in the highly anisotropic HTCS.[23,24,28,29] In the experimental situation of the Nb/Cu superlattices, i.e., a layered superconductor with magnetic field applied perpendicular to layers, one may distinguish between the in-plane VG correlation length $\xi_{VG\parallel}$, and the perpendicular one $\xi_{VG\perp}$ (along the vortex line).[4] The *quasi*-2D character of the glass transition was explained in HTCS assuming that anisotropy induces limited vortex length, that precludes $\xi_{VG\perp}$ to diverge.[23,24] Thus, when approaching T_g, only $\xi_{VG\parallel}$ diverges up to the macroscopic size of the sample, whereas $\xi_{VG\perp}$ would remain finite with nearly a constant value. This applies to Nb/Cu superlattices in the coupled regime. Following Yamasaki *et al.*[23] and Sefrioui *et al.*[24] we can estimate the upper limit for $\xi_{VG\perp}$ from the $I-V$ characteristics. Isotherms above T_g show up Ohmic behavior at low current level, but they become nonlinear above I_{nl}. At this current level, the work done by the Lorentz force to create vortex excitations equals the thermal energy, $J_{nl}\phi_0\xi_{VG\parallel}\xi_{VG\perp}=k_BT$.[4] We used the isotherm at the highest temperature within the critical region, in particular the one at $T=4.038$ K shown in Fig. 4(a), for which $J_{nl}\approx 125$ A cm^{-2}. The in-plane correlation length $\xi_{VG\parallel}$ should be larger than the mean intervortex distance $a_0=(\phi_0/\mu_0 H)^{1/2}\approx 130$ nm for $\mu_0 H=0.11$ T. In particular we assumed $\xi_{VG\parallel}>2a_0$, and thus we obtained $\xi_{VG\perp}$90 nm. That is, the correlation length along vortex line is limited well below the sample thickness ~300 nm. However, it may be longer than other relevant characteristic lengths, as the superlattice modulation length $\Lambda=40$ nm and the superconducting coherence length $\xi_{S\perp}(T)\approx 35$ nm. We have estimated the vortex length l in the regime where this superlattice is decoupled, in which we observed a *pure* 2D VG transition, with the work done by Lorentz force $J_{nl}\phi_0\xi_{VG\parallel}l=k_BT$.[27] Taking the isotherm at $T=2.150$ K [Fig. 5(a)], $J_{nl}\approx 80$ A cm^{-2}, and $\xi_{VG\parallel}>2a_0=150$ nm for $\mu_0 H=0.4$ T, we get $l<30$ nm. Therefore, the vortex length l is shorter than superlattice modulation length $\Lambda=40$ nm, and cannot be much longer than the coherence length at this T, $\xi_{S\perp}\approx 20$ nm. A picture emerges from those estimations, in which coherence length $\xi_{S\perp}$ and sample thickness d are the relevant length scales to which the correlation length along vortex line $\xi_{VG\perp}$ has to be

compared. The *quasi*-2D character of the glass transition in the coupled regime develops since $\xi_{VG\perp}$, longer that $\xi_{S\perp}$ is shorter than sample thickness d. At lower temperatures, Nb layers are decoupled by Cu ones. Therefore the vortex length l is limited by the modulation length Λ. Because of this, vortex length l and coherence length $\xi_{S\perp}$ get of similar magnitude, what yields a *pure* 2D VG transition. This is similar to what has been observed in highly anisotropic HTCS, for which *pure* 2D VG transitions have been observed when vortex length is limited to superconducting coherence length.[24,28,29]

To end up, we will discuss on the size of thermal displacement fluctuations of the vortex lines at the observed VG transition temperatures. Although the VG transition is completely different to a *melting* first order transition between *solid* and *liquid* vortex phases, one may use the Lindemann criterion yielding the melting line to roughly estimate the order-of-magnitude of the amplitude of thermal displacement fluctuations of vortices at T_g.[2,30] The *melting* takes place when the amplitude of thermal fluctuations is some fraction c_L (Lindemann number) of the vortex lattice parameter $\langle u^2\rangle_T = c_L^2 a_0^2$, with c_L system dependent and typically $\sim 0.2-0.3$ for HTCS. The related well-known expression for the melting line[2,30] is $h_m(1-h_m)^{-3} \approx (\pi/4) c_L^4 Gi^{-1}(1-t)t^{-2}$, where $h_m = H_m/H_{c2}$, $t = T/T_c$, the Ginsburg number $Gi = (T_c \sqrt{8}\varepsilon\varepsilon_0 \xi_{S\|})^2$ with the anisotropy $\varepsilon = \xi_{S\perp}/\xi_{S\|}$ and line energy $\varepsilon_0 = [\phi_0/4\pi\lambda_\|(0)]^2$, and $\lambda_\|(0)$ the penetration length at $T=0$. Using the sample parameters listed in Table I, we estimated c_L by introducing the experimental points $T_g(H)$ into the expression of the melting line. The results are also listed in Table I. The obtained c_L are in all cases $\sim 0.01-0.03$, in the range previously reported for vortex-lattice melting in Nb thin films.[13] This small Lindemann number means that the thermally induced displacement fluctuations of vortices needed to *melt* the vortex-lattice (or the VG) have amplitudes around one order-of-magnitude smaller than those observed in HTCS. On the other hand, the width of the critical region observed here for LTCS is much narrower. While for HTCS the critical region may spread several Kelvin, the width of the critical region observed here for LTCS is typically of some hundreds of milli-Kelvin i.e., for the LTCS the glass transition lies much closer to H_{c2} than for HTCS: typically, the parameter $[T_{Hc2} - T_g(H)]/T_{Hc2} \gtrapprox 0.1$ for HTCS (where T_{Hc2} is the temperature at which $H = H_{c2}$), while here we have observed $[T_{Hc2} - T_g(H)]/T_{Hc2} \sim 0.01$ for LTCS. Close to H_{c2} vortices are large objects (core size $\sim 2\xi_{S\|}$) compared to the mean vortex-lattice parameter a_0, and therefore in its vicinity the space between vortices is small. In this scenario small thermal displacement fluctuations of vortices are able to melt the vortex lattice (or glass).

IV. SUMMARY

We have shown evidence of the VG transition in the mixed state of Nb thin films and Nb/Cu superlattices by means of the scaling of $I-V$ characteristics. The VG transitions in these LTCS belong to the same universality generally found for HTCS systems, since the same critical exponents have been found. The glass transition lies much closer to H_{c2} in the low-temperature system, because of the small thermal fluctuations of in comparison to those in HTCS. The dimensionality of the VG transition has been investigated. While Nb thin films show up a 3D VG transition, a crossover from a *quasi*-2D into a *pure* 2D VG transition has been observed for Nb/Cu superlattices, which is governed by the ratio of the VG correlation length ξ_{VG} to the superconducting coherence length ξ_S.

ACKNOWLEDGMENTS

We acknowledge support from Spanish Ministerio de Educación y Ciencia under Grant Nos. MAT2002-04543 and MAT2002-12385-E, and the "Ramón Areces" Foundation. We would like to acknowledge Z. Sefrioui and J. Santamaria for helpful discussions.

[1] F. Bouquet, C. Marcenat, E. Steep, R. Calemczuk, W. K. Kwok, U. Welp, G. W. Crabtree, R. A. Fisher, N. E. Phillips, and A. Schilling, Nature (London) **411**, 449 (2001).

[2] G. Blatter, M. V. Feigel'man, V. B. Geshkenbein, A. I. Larkin, and V. M. Vinokur, Rev. Mod. Phys. **66**, 1125 (1994).

[3] M. P. A. Fisher, Phys. Rev. Lett. **62**, 1415 (1989).

[4] D. S. Fisher, M. P. A. Fisher, and D. A. Huse, Phys. Rev. B **43**, 130 (1991).

[5] P. W. Anderson and Y. B. Kim, Rev. Mod. Phys. **36**, 39 (1964).

[6] J. W. Lynn, N. Rosov, T. E. Grigereit, H. Zhang, and T. W. Clinton, Phys. Rev. Lett. **72**, 3413 (1994).

[7] P. L. Gammel, U. Yaron, A. P. Ramirez, D. J. Bishop, A. M. Chang, R. Ruel, L. N. Pfeiffer, E. Bucher, G. D'Anna, D. A. Huse, K. Mortensen, M. R. Eskildsen, and P. H. Kes, Phys. Rev. Lett. **80**, 833 (1998).

[8] X. S. Ling, S. R. Park, B. A. McClain, S. M. Choi, D. C. Dender, and J. W. Lynn, Phys. Rev. Lett. **86**, 712 (2001).

[9] S. R. Park, S. M. Choi, D. C. Dender, J. W. Lynn, and X. S. Ling, Phys. Rev. Lett. **91**, 167003 (2003).

[10] S. Okuma and N. Kokubo, Phys. Rev. B **56**, 14138 (1997).

[11] N.-C. Yeh, D. S. Reed, W. Jiang, U. Kriplani, C. C. Tsuei, C. C. Chi, and F. Holtzberg, Phys. Rev. Lett. **71**, 4043 (1993).

[12] S. Okuma, Y. Imamoto, and M. Morita, Phys. Rev. Lett. **86**, 3136 (2001).

[13] M. F. Schmidt, N. E. Israeloff, and A. M. Goldman, Phys. Rev. Lett. **70**, 2162 (1993).

[14] Y. Ando, H. Kubota, and S. Tanaka, Phys. Rev. B **48**, 7716 (1993).

[15] Young Sun, M. B. Salamon, K. Garnier, and R. S. Averback, Phys. Rev. Lett. **92**, 097002 (2004).

[16] C. S. L. Chun, G.-G. Zheng, J. L. Vicent, and I. K. Schuller, Phys. Rev. B **29**, 4915 (1984).

[17] D. R. Strachan, M. C. Sullivan, P. Fournier, S. P. Pai, T. Venkatesan, and C. J. Lobb, Phys. Rev. Lett. **87**, 067007 (2001).

[18] I. K. Schuller, Phys. Rev. Lett. **44**, 1597 (1980); J.-P. Locquet, D. Neerinck, L. Stockman, Y. Bruynseraede, and I. K. Schuller, Phys. Rev. B **38**, R3572 (1988); **39**, 13338 (1989).
[19] Eric E. Fullerton, I. K. Schuller, H. Vanderstraeten, and Y. Bruynseraede, Phys. Rev. B **45**, 9292 (1992).
[20] R. H. Koch, V. Foglietti, W. J. Gallagher, G. Koren, A. Gupta, and M. P. A. Fisher, Phys. Rev. Lett. **63**, 1511 (1989).
[21] P. J. M. Wöltgens, C. Dekker, R. H. Koch, B. W. Hussey, and A. Gupta, Phys. Rev. B **52**, 4536 (1995).
[22] P. Voss-deHaan, G. Jakob, and H. Adrian, Phys. Rev. B **60**, 12 443 (1999).
[23] H. Yamasaki, K. Endo, S. Kosaka, M. Umeda, S. Yoshida, and K. Kajimura, Phys. Rev. B **50**, 12959 (1994).
[24] Z. Sefrioui, D. Arias, M. Varela, J. E. Villegas, M. A. López de la Torre, C. León, G. D. Loos, and J. Santamaría, Phys. Rev. B **60**, 15423 (1999).
[25] E. M. Gonzalez, E. M. Luna, Z. Sefrioui, J. Santamaria, and J. L. Vicent, J. Low Temp. Phys. **117**, 675 (1999).
[26] Katerina Moloni, Mark Friesen, Shi Li, Victor Souw, P. Metcalf and M. McElfresh, Phys. Rev. B **56**, 14784 (1997).
[27] C. Dekker, P. J. M. Wöltgens, R. H. Koch, B. W. Hussey, and A. Gupta, Phys. Rev. Lett. **69**, 2717 (1992).
[28] H.-H. Wen, H. A. Radovan, F.-M. Kamm, P. Ziemann,. S. L. Yan, L. Fang, and M. S. Si, Phys. Rev. Lett. **80**, 3859 (1998).
[29] Z. Sefrioui, D. Arias, M. Varela, M. A. López de la Torre, C. León, G. D. Loos, and J. Santamaría, Europhys. Lett. **48**, 679 (1999).
[30] J. Kierfeld and V. Vinokur, Phys. Rev. B **69**, 024501 (2004).
[31] J. Guimpel, F. de la Cruz, J. Murduck, and I. K. Schuller, Phys. Rev. B **35**, R3655 (1987).